Energy Equip. Sys./ Vol. 13/No. 2/June 2025/ 147-166

ENERGY EQUIPSYS

Energy Equipment and Systems

www.energyequipsys.com

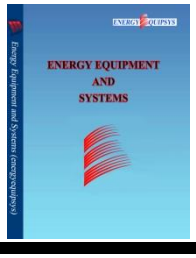

Comparative experimental analysis and correlation development for pressure drop in vertical helical tubes with non-boiling air/water two-phase flow in both upward and downward directions

Article Type
Research

Authors

Ayat Sabatsany[a]
Rogayyeh Motallebzadeh[a*]
Samad Jafarmadar[b]
Adolsalam Ebrahimpour[a]

[a] Department of Mechanical Engineering, Tabriz Branch, Islamic Azad University, Tabriz, Iran

[b] Department of Mechanical Engineering, Faculty of Engineering, Urmia University, Urmia, Iran

Article history:

Received : 3 August 2024
Revised:25 August 2024
Accepted : 9 September 2024

ABSTRACT

Helical tubes are very efficient and stable in managing two-phase flows, thanks to their tightly coiled structure. Additionally, their thermal performance is commendable. Expanding our understanding of the thermal and entropic properties of two-phase flows in helical tubes is of the utmost importance due to the widespread use of these flows in many applications. This study intends to conduct experimental investigations into the hydrodynamic properties of helical tubes. The research included putting various sized coil tubes through their paces using a two-phase air/water flow. A vertical helical tube with coils of varied diameters was used to achieve this objective. After being properly mixed in a mixing chamber, the water and air are sent into the helical pipe, where they flow downward and upward. This study primarily examines the impact of lowering pressure. The major emphasis of this study is to use multiple linear regression to assess the gathered experimental data and generate a correlation for pressure loss. In downhill flow, the findings show that a smaller coil diameter leads to a lower pressure drop, but in upward flow, the opposite is true. The minimum value of pressure drop is 170.75 and 133.45 for upward and downhill flow respectively. In addition, in a downhill flow, the maximum pressure drop ratio is around 1.25, while in an upward flow, it is 1.63.

Keywords: Two Phase Flow, Helix Coil, Pressure Drop Correlation, Downward Flow, Upward Flow.

1. Introduction

Heat exchangers play a vital role in industrial equipment. Currently, helical tubes are often used in small heat exchangers, as well as in associated equipment like evaporators and freezers. Various industrial sectors, including heat exchangers, evaporators, freezers, nuclear reactors, pharmaceuticals, biotech, food and beverage, automotive, aerospace, and the oil and gas industry, encounter the issue of pressure drop in vertical helical tubes with non-boiling two-phase air/water flow. Helical tubes are widely esteemed in these domains due to their outstanding thermal efficiency and compactness. Accurate knowledge of pressure drop enables the enhancement of

* Corresponding author: Rogayyeh Motallebzadeh
Department of Mechanical Engineering, Tabriz Branch, Islamic Azad University, Tabriz, Iran
Email: Motallebzadeh@iaut.ac.ir

design and operation in refrigeration systems and compact heat exchangers, resulting in improved efficiency and reduced operating expenses. Effective pressure drop control is crucial in the oil and gas sector to prevent flow assurance issues, improve separation processes, and ensure efficient transportation of oil and gas mixtures. Helical tubes are essential for ensuring the safety and efficiency of nuclear reactors by facilitating the safe and efficient transfer of heat. Furthermore, having precise knowledge of the extent of pressure decrease is essential for the biotech and pharmaceutical industries to maintain consistent operations, hence ensuring the quality and reliability of their goods. Ensuring the smooth and efficient implementation of thermal processes, such as pasteurization and sterilization, is of utmost importance in the food and beverage industry to guarantee the safety and quality of the goods. Helical tube heat exchangers are used in chemical processing facilities, as well as in the automotive and aerospace industries, to provide effective heat transfer and process management. They are particularly useful in cooling systems. A comprehensive understanding of pressure drops in helical tubes leads to many benefits, including energy savings, cost reduction, enhanced safety, and improved performance across several industries. This knowledge enables the construction of more reliable and efficient systems. Therefore, the pursuit of different strategies to improve their effectiveness is very important in this industry [1–3]. The study undertaken by Fsadni et al. [4] emphasizes the limited amount of research that has been done on the hydrodynamics of two-phase non-boiling flows in helical pipes. Helical pipes are more complex than smooth tubes because to their enhanced heat transfer efficiency, suitable construction, exceptional compaction, flow stability, and the influence of centrifugal forces in vertical configurations [5]. An adaptive neuro-fuzzy inference method was used by Mehrabi et al. [6] to model the pressure drop and heat transfer coefficient in the inner and annular regions. Incorporating parameters like the Prandtl number, coil pitch, and Dean number, they compared their results to experimental data. Using a genetic algorithm, Mehrabi et al. [7] investigated many heat transport components. Statistical criteria were used for the comparison of the results. Experimental research was carried out by Khorasani et al. [8] to investigate the effect of geometric properties on thermal performance of helically curved wires used as tabulators. They discovered that the pitch and wire diameter affect the Nusselt number and friction factor. Furthermore, an experimental investigation was carried out by Khorasani et al. [9] to ascertain the efficacy of a helical-shaped shell and coiled heat exchanger when horizontally oriented air bubbles were introduced. A lot of studies have tried to figure out what makes helical and smooth tube flow patterns different. Three separate flow regimes, including ascending and descending bubble flows, slug flows, and two-phase flows in different tube designs (horizontal, vertical, angular, and helical), have been repeatedly shown by these studies [10]. The spiral-shaped tube utilized by Aliabadi and Feizabadi [11] has a corrugated surface. Their findings suggest that a wavy shape, when applied to helical tubes, might increase the turbulence intensity of the flow, leading to a possible 46% index jump. In their research, Mousavi et al. [12] investigated the incorporation of air into a vertical shell that was fitted with a coil. A heat exchanger was used, using coiled tubes to augment heat transfer. Specialized modeling methods were used by researchers to illustrate the adaptation of helical tube data. Pashaee and Pesteei [13] performed a numerical analysis on a double-tube coiled heat exchanger to assess the influence of the Dean Number and curvature ratio on pressure drop and heat transfer coefficient. Guo et al. [14] predicted the level of dryness in the two-phase flow characteristics inside a helically coiled pipe at four distinct axial orientations. Taha et al. [15] compared experimental and computational findings on the motion of Taylor bubbles, distribution of velocities, and local wall shear stress. After calculating the distributions of local wall shear stress and velocity, they were compared to empirical research. Slug and bubble flows in helical pipes were studied by Murai et al. [16], who discovered that centrifugal forces impact the flow pattern. The nonlinear vibration of pipes with two-phase flow and heat flux was studied by Adegoke et al. [17]. According to the results, the critical velocity increases as the void percentage rises. By simulating a two-phase flow numerically, Hossain et al. [18] showed that the

slug and churn flows' frequency of volume fraction changes matched very well. In a computer study, Akhlaghi et al. [19] modelled the plug and slug flow regimes in a 44 mm diameter horizontal pipe. They used the SST k-ε model and a model for multiple fluid volumes. To study two-phase flow, Mimouni et al. [20] presented a multifield method based on the two-fluid model. Using data from three separate experiments, they proved their model was correct. Using theoretical, computational, and experimental methods, Malekzadeh et al. [21] investigated severe slugging in a lengthy pipeline-riser system in detail. There was a horizontal steel pipeline connected to an angled Perspex pipeline, a vertical PVC riser after that. Air and water served as the working fluids of the pipeline, which was designed to function at atmospheric pressure. Beyond that. A two-fluid model with one dimension was used to run a numerical simulation. In their experiment, Xie et al. [22] used a pipeline-riser system with a 300bar maximum pressure. According to their findings, the region of intense slugging shrank as the backpressure on the flow pattern map rose. Pressure drop and heat transfer coefficient were thoroughly examined by Onal et al. [23], who took into account several aspects such as coil pitch, diameter, heat flux, mass flow, and more. A numerical investigation on an exchanger with a helical form was carried out by Fan et al. [24] using the RNG k-ε turbulence model. When comparing eccentric and concentric cases, they discovered notable variations in the flow field and heat transmission. Dhenge et al. [25] used helical pipes in a high-pressure technique to analyze orange juice. Fluid flow in a helix was the subject of an experimental investigation by Lei and Bao [26]. They were able to establish a link in the end. Using experimental data from various fuels and designs, this research verified the connection. Seventeen helical-shaped coiled tubes with different inner and coil diameters, inclination angles, and operation conditions were the subject of an experimental study by Xu et al. [27]. A correlation was reported and compared with experimental data acquired in the open literature as part of their inquiry. In their study, Moaf et al. [28] looked at how downflow helix tubes' thermal efficiency changed when air was injected into them. Researchers briefly analyzed pressure drop to get the C.B.R. factor; nonetheless, thermal performance is the major emphasis of the study. In their study, Eliyasi and Farhadi [29] suggested having An interactive computer program is offered for these calculations and predictions, as well as a new analytical relation that consistently predicts two-phase gas-liquid flow patterns in horizontal pipes. This relation is based on Kern's pressure drop calculation technique and a modified Baker diagram. Zare Aliabadi et al. [30] conducted an experiment on a gas-liquid thermosyphon heat exchanger (THE) and discovered that the ε-NTU approach accurately forecasts heat transfer and pressure drop. They also discovered a novel correlation that achieved an error of less than 15% across 40 experimental points. In a study conducted by Zare Aliabadi et al. [31], experimental data was used to validate the accuracy of the computational fluid dynamics (CFD) models of the temperature distribution and thermal performance. The study examined a gas-liquid thermosyphon heat exchanger with integrated heat pipes and aluminum plate fins. A large-scale experimental examination on spiral-wound heat exchangers (SWHEs) was carried out by Wnag et al., who found that the frictional pressure drop increases with total mass flow rate and vapor quality. [32] The experimental results could be accurately predicted, to within ±25% accuracy, using a modified correlation for pressure losses. A novel vibrating woven wire turbulator may increase heat transfer efficiency in heat exchangers by 236%, according to research by Khedher et al. [33]. When coupled with a helical coiled wire turbulator, this turbulator achieves a TEF of 3.13, a marginal pressure drop increase of 1%, and a TEF of 2.45. Marzouk et al. [34] investigated the thermal and hydraulic performance of a helical tube heat exchanger (HTHE) using various tube configurations. They tested six designs, finding that HTHE6 offered the highest heat transfer enhancement (125–185%) and exergy efficiency, while pressure drop increased with Reynolds number. The study concluded that novel tube arrangements significantly improve heat transfer with minimal impact on pressure drop and pumping power. Kia et al. [35] investigated the heat transfer and pressure drop of Al_2O_3 and SiO_2 nanofluids in a helical tube under constant heat flux. They found that nanofluids significantly improved heat transfer and increased pressure drop compared to

the base oil, with Al_2O_3 outperforming SiO_2. The highest enhancement was at 0.5% concentration, where Al_2O_3 and SiO_2 increased heat transfer by 41.4% and 27.3%, respectively. Using a helical tube improved heat transfer by 19.5%, with additional gains from reducing the helical pitch and pitch circle diameter. Zheng et al. [36] investigated friction pressure drop and circumferential heat transfer in helical tubes, commonly used in nuclear and refrigeration systems. They found that coil diameter significantly impacts pressure drop and heat transfer uniformity, with the outer tube wall showing the highest heat transfer, especially in smaller coils. The study also introduced improved correlations for predicting flow resistance and heat transfer in both single-phase and two-phase flows. Kumar et al. [37] experimentally studied flow boiling in a helical coil under subatmospheric pressure. They found that two-phase pressure drop is higher at subatmospheric pressure compared to atmospheric, especially at higher mass flux and vapor quality. The pressure drop increased linearly with heat flux, and existing correlations accurately predicted the pressure drop data.

So far, no comprehensive study has used experimental, computational, or analytical approaches to probe the hydrodynamic behavior of air/water flow in a helical tube. Therefore, there is a dearth of trustworthy experimental evidence to build correlations for forecasting pressure drop values. So, to prove the connection over a wide range of flow rates, this study is carried out experimentally. In addition to studying the downward movement, the two-phase flow causes the internal pipe flow to increase. Ultimately, a correlation equation is developed that applies to both uphill and downhill flows. For the first time, the pressure drop experiments are used to generate a correlation equation, which may serve as a foundation for future investigations. The innovations and objectives of the present study are summarized as follows:

- Detailed analysis of coil diameter effects on pressure drop.
- Comparison of pressure drops in upward vs. downward flow.
- Providing a correlation equation for uphill and downhill flows.

Nomenclature

D	Diameter, mm
VF	volume fraction
P	Static pressure, pa
Q	Volume flow rate, lit/min
Re	Reynolds number
u	Velocity, m/s
MR	Multiple correlation coefficient

Greek symbols

ρ	Density, kg/m^3
μ	Dynamic viscosity, Pa.s

2. Experiments procedure

The current investigation included a controlled experiment that followed the procedures laid forth by Moradi et al. [38]. Within a dedicated mixing chamber, two main flows meet in this configuration. The airflow is controlled by a KHL-08A01M-V rotameter, which detects the flow rate accurately and modifies it via two control valves. The compressor is a standard model. Two valves on the main and bypass lines allow for the modification of the flow rate, which is controlled by a pre-filled tank that supplies the water. The volumetric flow rate of the water is accurately measured by an additional rotameter. Once everything is mixed up in the chamber, the water is piped into the test area to mix with the airflow. Optimal positioning of pressure monitoring devices at the tube's intake and outflow permits accurate detection of pressure differentials throughout the system. A computerized manometer and data recorder work together to do this, guaranteeing precise readings. The experimental setup and tubes are schematically shown in Figus. 1 and 2, which serve as visual guides to the system's structure. To fully grasp the research, the dimensions and specifications of the setup are detailed in Table 1, which also includes the geometric qualities that were crucial.

The helical tubes that were used for this research are shown in Fig. 1. The helical form has a special impact on the system's pressure drop and heat transmission properties due to the secondary flow patterns it creates. The study's overarching goal is to investigate, under varied flow circumstances, the effect of various geometric configurations on the system's performance utilizing helical tubes of varied

sizes. The inner diameter of the tube is fixed at 10 mm for all the tubes used in the experiments. The inner diameter is crucial as it directly influences the flow rate and the frictional characteristics within the tube. The tubes are configured with three different coil diameters: 100 mm, 140 mm, and 180 mm. The coil diameter affects the curvature of the helical tube, which in turn impacts the centrifugal forces acting on the fluid and the secondary flow patterns. All the tubes have 5 loops. The number of loops determines the length of the helical path the fluid has to traverse, affecting the overall pressure drop and flow distribution. The pitch of the helix is 70 mm. This parameter defines the axial distance between successive turns of the helix and influences the compactness of the coil and the interaction between adjacent turns.

The current state of the experiment is shown in Table 3. The study investigates four unique water flow rates and four unique air flow rates, guaranteeing that each water flow rate is exposed to four different air flow rates, and vice versa. The two streams of water and air are merged in the mixing chamber and sent into a tube with three distinct coil diameters (100, 140, and 180 mm) in both upward and downward orientations.

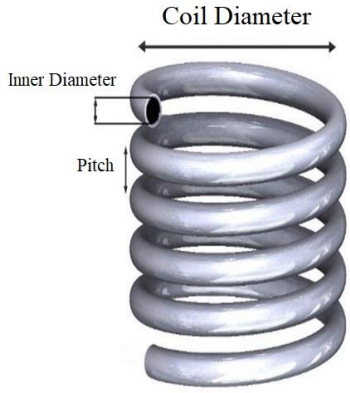

Fig. 1. Helical tubes used in the experiments.

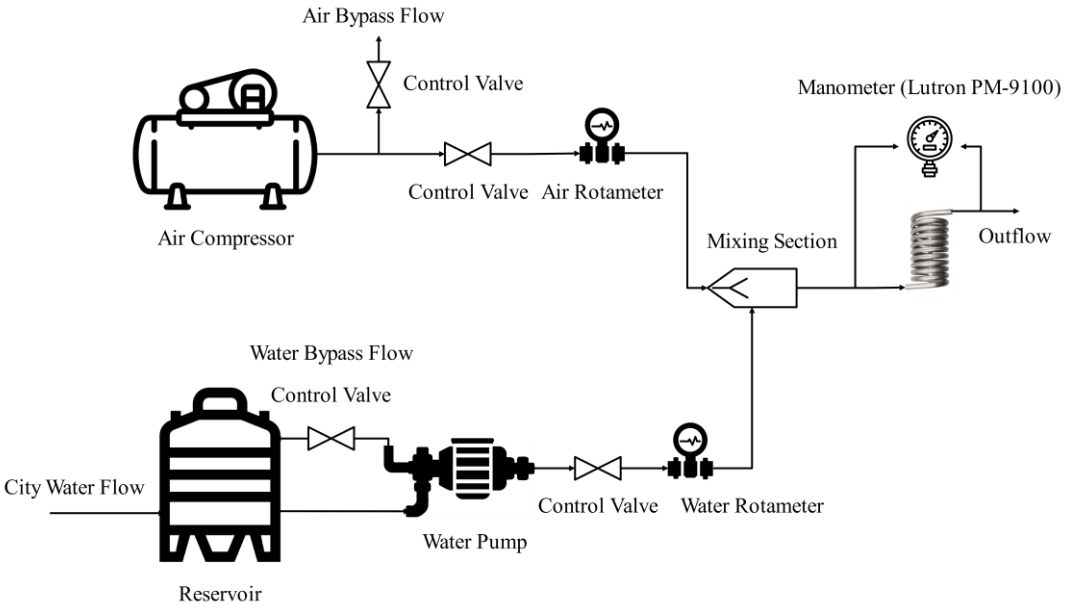

Fig. 2. Graphical representation of the experimental setup.

Table 1. The geometric characteristics of the tube.

Inner diameter of tube (mm)	Coil diameter (mm)	Loops	Helix pitch (mm)
10	100, 140, 180	5	70

Table 2. The accuracy of the equipment used in the experimental setup.

Equipment	Model	Accuracy
Rotameter	KHL-08A01M-V	±1-5%
Manometer	Lutron PM-9100	±0.3%

Table 3. Status of the experiment.

Air flow rate (Lit/min)	Water flow rate (Lit/min)	Flow direction
1, 3, 5, 7	2, 4, 6, 8	downward/upward
1, 3, 5, 7	2, 4, 6, 8	downward/upward
1, 3, 5, 7	2, 4, 6, 8	downward/upward

3. Correlation Extraction

Linear regression, a popular statistical tool for modeling the connection between variables, will be used to analyze the data. In this context, the significance of a value (referred to as "Y" in the dependent variable) is examined by analyzing its correlation with one or more values (referred to as "X" in the independent variables) that explain it. The forecast of "Y" may be represented by specifying three potential values for "X":

$$Y = B_0 + B_1X_1 + B_2X_2 + B_3X_3 \quad (1)$$

Equation 1 makes use of the experimental data shown in Table 4, which were derived from the testing. Fig. 4 illustrates the fitting of predicted plots and Actual Ys, whereas Fig. 3 presents the variables' residuals. A normal probability map of the experimental data is shown in Fig. 15.

Table 4. Experimental data used to extract correlation for downward flow.

	X Variable 1	X Variable 2	X Variable 3	Y
No.	Coil Diameter [m] (D)	Air mass flow rate [lit/min] (Q_g)	Volume fraction (VF)	Pressure loss [mbar]
1	0.18	1	0.1	375.83
2	0.18	1	0.15	311.22
3	0.18	1	0.2	255.80
4	0.18	1	0.3	155.61
5	0.18	3	0.25	386.73
6	0.18	3	0.3	320.25
7	0.18	3	0.43	263.10
8	0.18	3	0.6	160.12
9	0.18	5	0.39	395.05
10	0.18	5	0.45	326.97
11	0.18	5	0.55	267.95
12	0.18	5	0.72	163.49
13	0.18	7	0.46	402.35
14	0.18	7	0.54	333.18
15	0.18	7	0.64	273.25
16	0.18	7	0.77	166.59
17	0.14	1	0.1	341.93
18	0.14	1	0.15	283.21
19	0.14	1	0.2	232.78
20	0.14	1	0.3	141.61
21	0.14	3	0.25	352.27
22	0.14	3	0.3	291.71
23	0.14	3	0.43	239.76

No.	X Variable 1 Coil Diameter [m] (D)	X Variable 2 Air mass flow rate [lit/min] (Q_g)	X Variable 3 Volume fraction (VF)	Y Pressure loss [mbar]
24	0.14	3	0.6	145.85
25	0.14	5	0.39	362.83
26	0.14	5	0.45	300.46
27	0.14	5	0.55	247.33
28	0.14	5	0.72	150.23
29	0.14	7	0.46	370.09
30	0.14	7	0.54	307.40
31	0.14	7	0.64	251.89
32	0.14	7	0.77	153.23
33	0.1	1	0.1	322.41
34	0.1	1	0.15	266.22
35	0.1	1	0.2	218.27
36	0.1	1	0.3	133.45
37	0.1	3	0.25	336.31
38	0.1	3	0.3	276.87
39	0.1	3	0.43	227.56
40	0.1	3	0.6	138.79
41	0.1	5	0.39	345.37
42	0.1	5	0.45	285.17
43	0.1	5	0.55	234.39
44	0.1	5	0.72	142.95
45	0.1	7	0.46	352.27
46	0.1	7	0.54	290.88
47	0.1	7	0.64	239.08
48	0.1	7	0.77	146.05

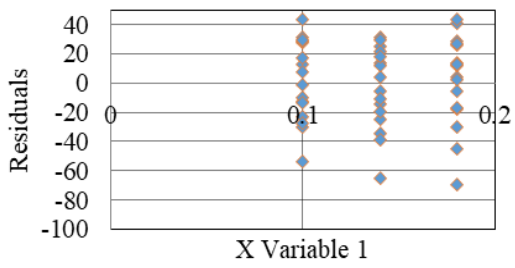

(a)

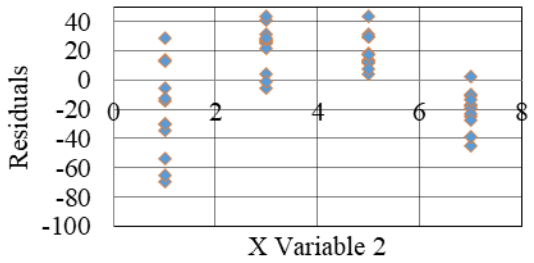

(b)

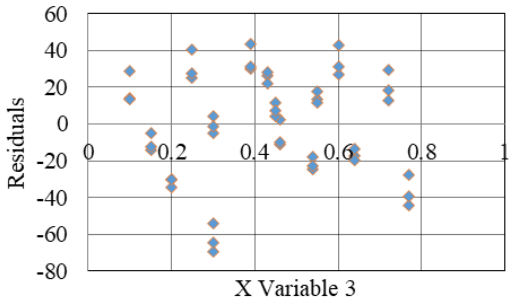

(c)

Fig. 3. Residuals plots for downward flow, (a) X Variable 1, (b) X Variable 2, (c) X Variable 3.

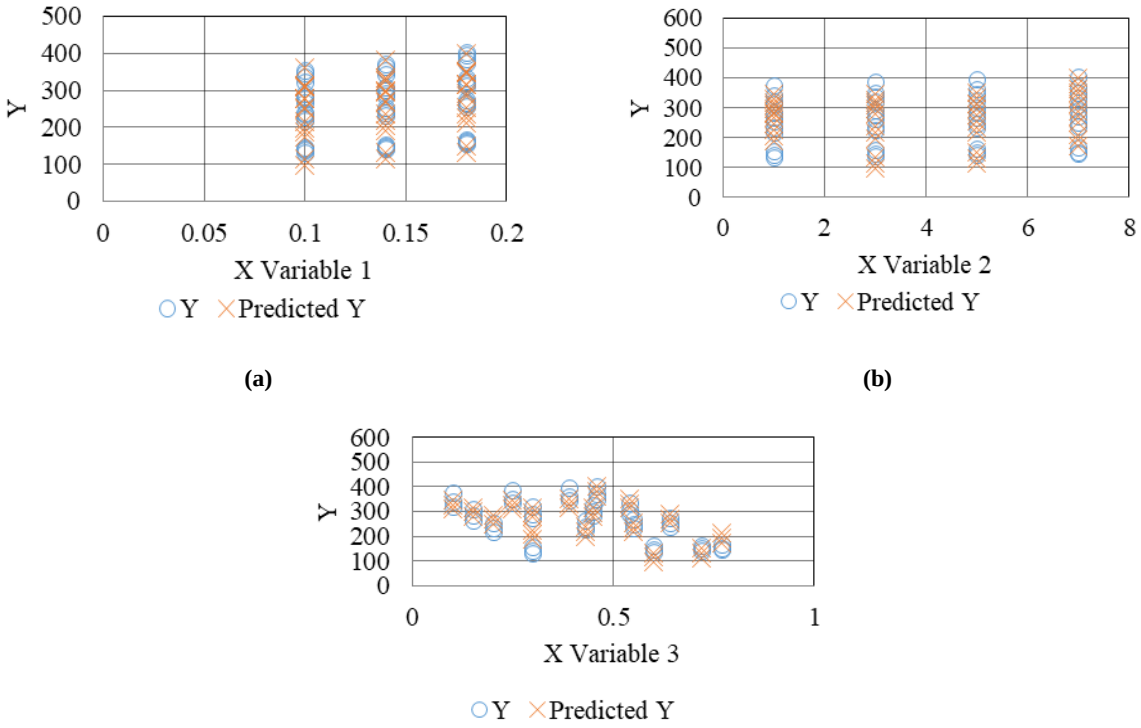

Fig. 4. The fitting of predicted plots and actual Ys. For downward flow, (a) X Variable 1, (b) X Variable 2, (c) X Variable 3.

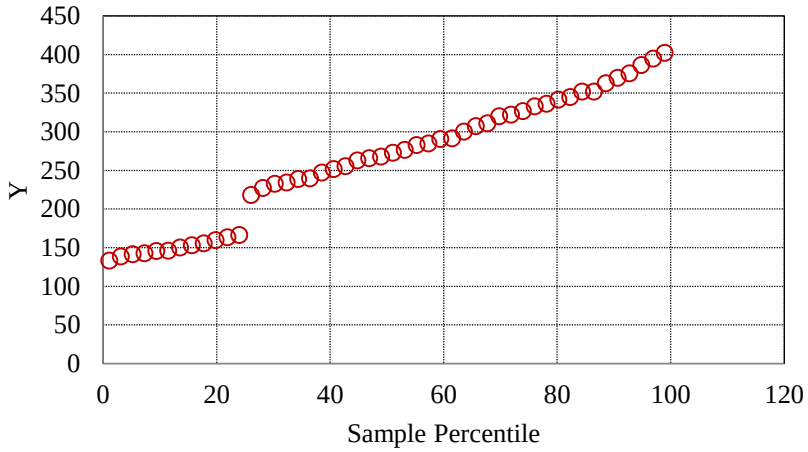

Fig. 5. Normal Probability Plot for downward flow.

The "Error" here is the sum of squares of the data points' deviation from the regression line, which is the actual data points. In Table 5, you can see the results of the regression analysis.

The results are used to generate the following equation for downhill flow correlation:

$$\Delta P = 45.3455\left[6.12 + 10.36D + Qg - 13.42VF\right] \quad (2)$$

The same linear regression method is applied to analyze the data for upward flow using the values presented in Table 6. This approach allows us to predict "Y" for the upward flow scenario, leveraging the experimental data from Table 5 to ensure the model's accuracy and reliability.

Table 5. Regression Statistics for downward flow.

MR	0.936012
R Square	0.876118
Adjusted R Square	0.867671
Standard Error	29.36632
Observations	48

Table 6. Achieved experimental data used to extract correlation for upward flow.

No.	X Variable 1 Coil Diameter [m] (D)	X Variable 2 Air mass flow rate [lit/min] (Q_g)	X Variable 3 Volume fraction (VF)	Y Pressure loss [mbar]
1	0.18	1	0.1	413.84
2	0.18	1	0.15	342.27
3	0.18	1	0.2	279.63
4	0.18	1	0.3	170.75
5	0.18	3	0.25	450.00
6	0.18	3	0.3	339.26
7	0.18	3	0.43	280.55
8	0.18	3	0.6	178.30
9	0.18	5	0.39	490.00
10	0.18	5	0.45	362.40
11	0.18	5	0.55	304.63
12	0.18	5	0.72	179.71
13	0.18	7	0.46	541.00
14	0.18	7	0.54	400.00
15	0.18	7	0.64	310.00
16	0.18	7	0.77	177.30
17	0.14	1	0.1	550.00
18	0.14	1	0.15	440.00
19	0.14	1	0.2	328.30
20	0.14	1	0.3	208.90
21	0.14	3	0.25	535.70
22	0.14	3	0.3	418.19
23	0.14	3	0.43	346.48
24	0.14	3	0.6	219.80
25	0.14	5	0.39	720.00
26	0.14	5	0.45	510.00
27	0.14	5	0.55	389.50
28	0.14	5	0.72	238.00
29	0.14	7	0.46	800.00
30	0.14	7	0.54	550.00
31	0.14	7	0.64	400.30
32	0.14	7	0.77	239.70
33	0.1	1	0.1	695.30
34	0.1	1	0.15	585.00
35	0.1	1	0.2	405.30
36	0.1	1	0.3	255.60
37	0.1	3	0.25	730.10
38	0.1	3	0.3	610.00
39	0.1	3	0.43	410.60
40	0.1	3	0.6	265.00
41	0.1	5	0.39	990.50
42	0.1	5	0.45	680.00
43	0.1	5	0.55	490.30
44	0.1	5	0.72	280.60
45	0.1	7	0.46	1080.60
46	0.1	7	0.54	726.30
47	0.1	7	0.64	512.30
48	0.1	7	0.77	310.60

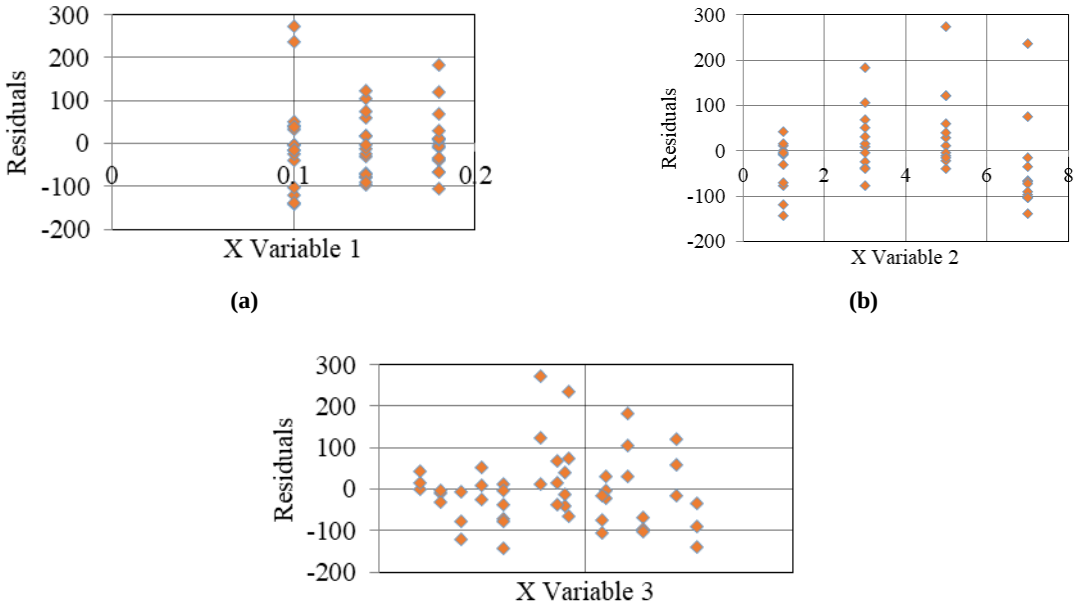

(a) **(b)**

(c)

Fig. 6. Residuals plots for all variables for upward flow,
(a) X Variable 1, (b) X Variable 2, (c) X Variable 3.

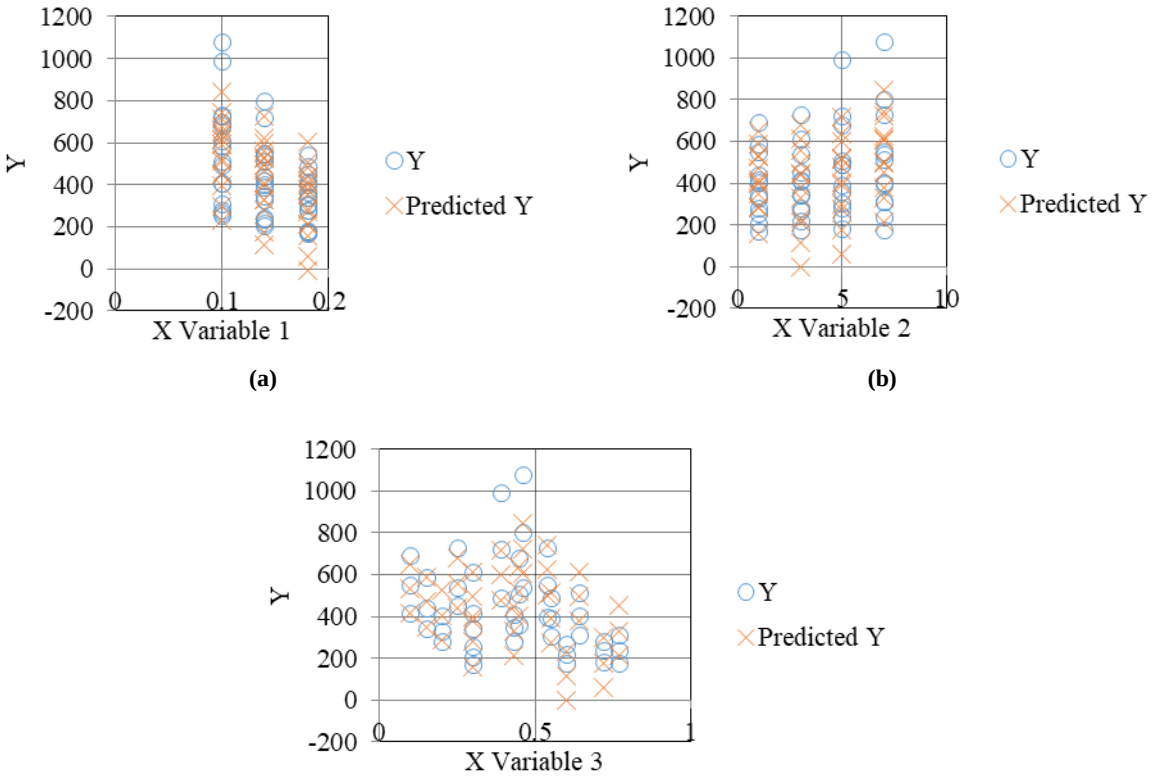

(a) **(b)**

(c)

Fig. 7. The fitting of predicted plots and actual Ys. For upward flow
(a) X Variable 1, (b) X Variable 2, (c) X Variable 3.

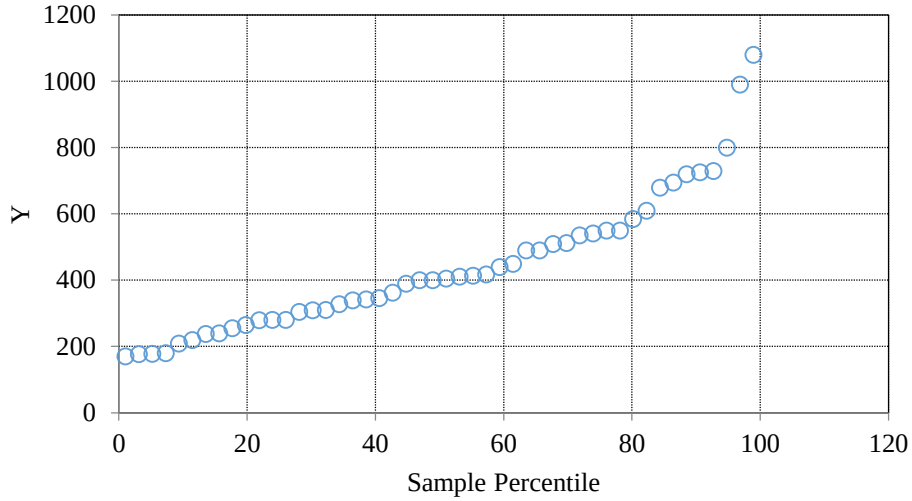

Fig. 8. Normal Probability Plot for upward flow.

Table 7. Regression Statistics for upward flow.

MR	0.906719894
R Square	0.822140967
Adjusted R Square	0.810014215
Standard Error	90.55592437
Observations	48

The following is a definition of the correlation based on the gathered results for predicting pressure loss in upward flow:

$$\Delta P = 108.34\left[8.94 - \left(27.46D - Qg + 11.74VF\right)\right] \quad (3)$$

4. Results and Discussion

Figures 9 to 14 show the data acquired from the tests, graphed for various diameters of 180, 140, and 100 mm, with both downward and upward flows. These charts compare the test results with the correlation equation derived in the preceding section. It should be mentioned that VF is defined as the ratio of Q_g to the total of Q_g and Q_l, where Q_g is the volume flow rate of gas and Q_l is the volume flow rate of water. Reducing the water flow rate or increasing the volume percentage both lower the pressure drop values. Increasing the water flow rate causes friction, which in turn causes higher pressure loss. Research has shown that when coil diameter is increased, downhill flow pressure drop values are increased, and uphill flow pressure drop values are decreased. The impact of centrifugal forces is responsible for this. A package going over a curved road will experience more effective centrifugal forces if the curvature diameter of the road is reduced. When a liquid is forced through a helical tube, the centrifugal forces acting upon it are proportionate to the secondary flow intensity. Consequently, streams that are perpendicular to the primary flow direction become stronger. As a result, the pressure drop increases, and the flow disturbances become more severe. If the flow conditions can be reliably and consistently measured over a 5-minute period, then the total pressure drop may be determined by averaging the highest and lowest readings. In particular, the maximum pressure drops for the downward-flowing streams are approximately 352, 370, and 402 mbar, and for the upward flowing streams they are approximately 1080, 800, and 541 mbar for the 100 mm, 140 mm, and 180 mm coils, respectively. Since the pressure drops across the mixed gas and liquid streams show fluctuating behavior, the results are presented as average values.

Across all figures, the experimental data align well with the theoretical equation derived previously. This validates the model and suggests it accurately predicts the pressure loss for varying conditions of flow direction and coil diameter. While the general trend of ΔP with VF holds for both upward and downward flows,

the exact values and slopes may vary slightly due to the different dynamics involved in upward versus downward flows. In summary, the experimental data presented in Figs. 9 to 14 demonstrate a strong correlation with the theoretical predictions, confirming that the model accurately captures the relationship between pressure loss, volume fraction, and coil diameter for both upward and downward flows.

For a coil diameter of 180 mm, Fig. 9, as the volume fraction increases, the pressure drop also increases. This trend indicates that the larger diameter allows for a more significant impact of the volume fraction on the pressure drop.

With a coil diameter of 140 mm, Fig. 10, a similar trend is observed, but the pressure drop values are higher compared to the 180 mm coil. This suggests that the reduction in coil diameter increases the resistance to flow.

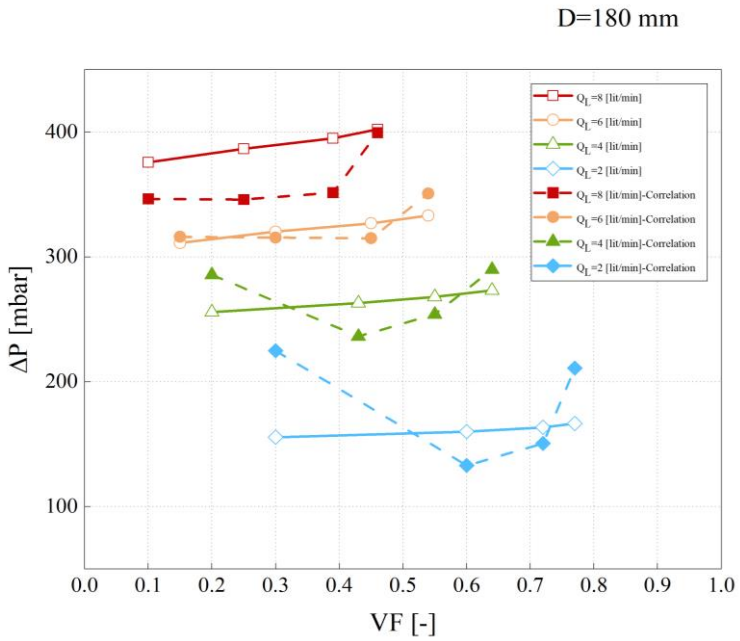

Fig. 9. Variation of ΔP vs. VF for D=180 mm, downward flow.

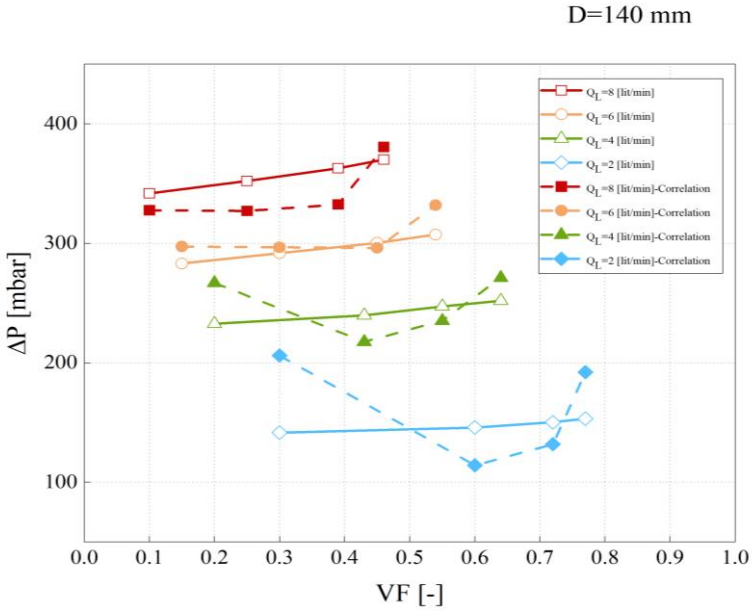

Fig. 10. Variation of ΔP vs. VF for D=140 mm, downward flow.

For the smallest coil diameter of 100 mm, Fig. 11, the pressure drop increases sharply with an increase in volume fraction, indicating the highest resistance among the tested diameters.

In the upward flow for a coil diameter of 180 mm, Fig. 12, the pressure drop increases with the volume fraction, but the values are generally higher than those in the downward flow due to the additional gravitational effects.

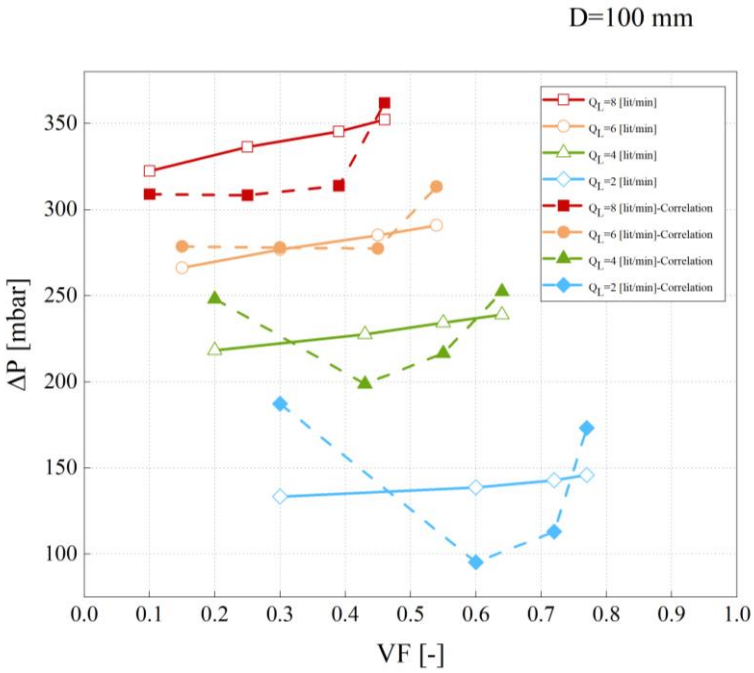

Fig. 11. Variation of ΔP vs. VF for D=100 mm, downward flow.

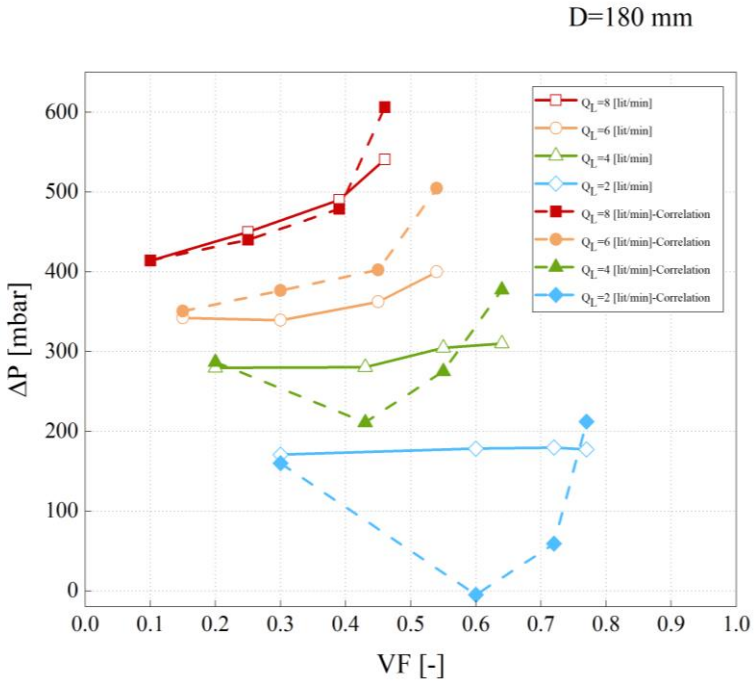

Fig. 12. Variation of ΔP vs. VF for D=180 mm, upward flow.

For a 140 mm coil diameter, Fig. 13, the pressure drop shows a similar increasing trend with volume fraction, with higher values compared to the downward flow for the same diameter.

The 100 mm coil diameter, Fig. 14, exhibits the highest pressure drop in the upward flow, demonstrating the significant impact of the smallest coil diameter in resisting the flow.

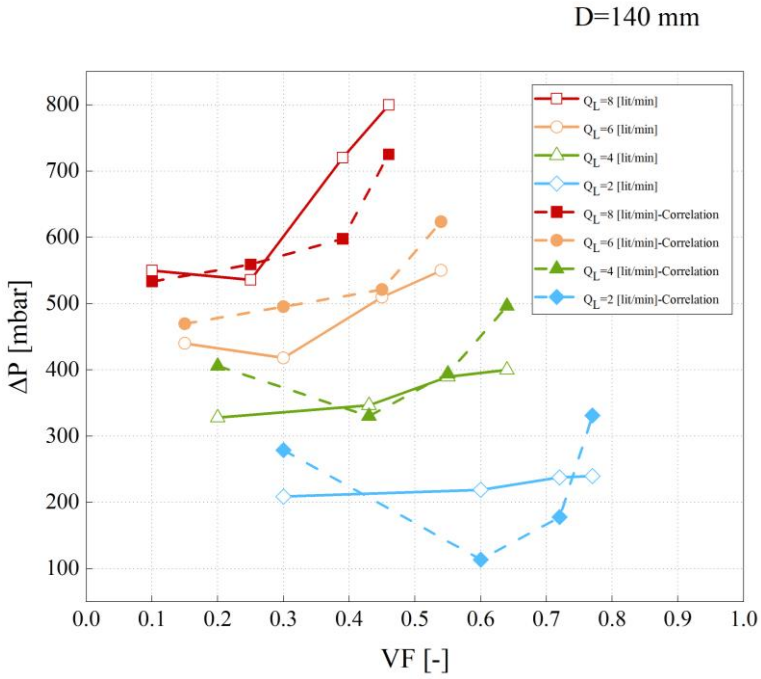

Fig. 13. Variation of ΔP vs. VF for D=140 mm, upward flow.

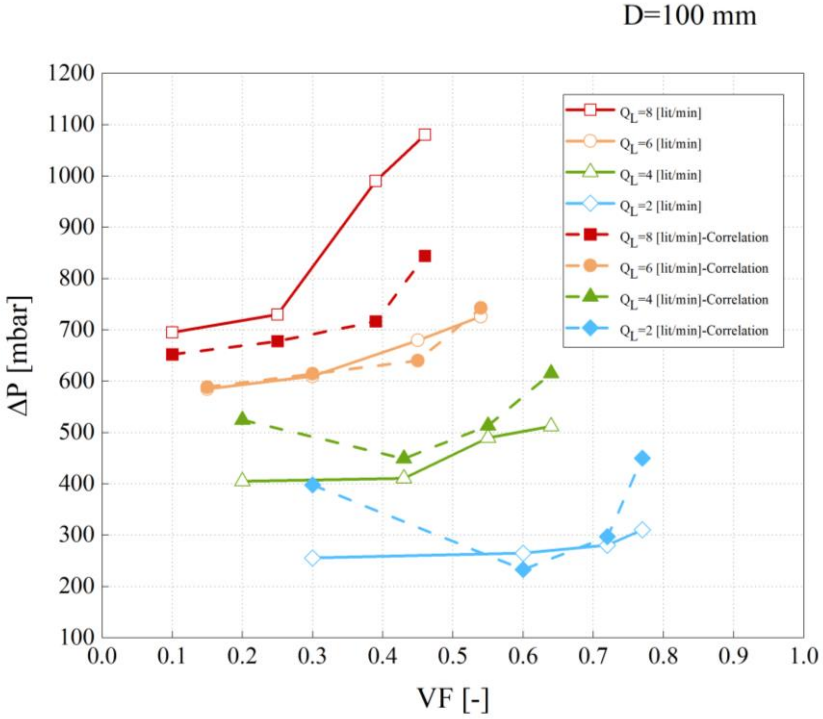

Fig. 14. Variation of ΔP vs. VF for D=100 mm, upward flow.

The data presented in these figures demonstrate a strong correlation with the theoretical predictions, confirming that the model accurately captures the relationship between pressure loss, volume fraction, and coil diameter for both upward and downward flows. Also, it is possible to compare the pressure drop for different coil diameters and in different flow directions in constant VF number. These data help the researchers to choose the correct coil size and flow direction according to their facilities in industry and laboratories. The general trends of the figures demonstrated that the pressure drop increases in the case of developing Q_g in constant values of Q_l.

4.1. Comparison of Upward and Downward Flows for Different Diameters

This section presents a comparison of pressure decreases in uphill and downhill flows for coil diameters of 180 mm, 140 mm, and 100 mm based on experimental test findings. In Fig. 15, the pressure drop (ΔP) is plotted against the volume fraction (VF) for both upward and downward flows with a coil diameter of 180 mm. The results indicate that the pressure drop is generally higher in the upward flow compared to the downward flow for the same volume fraction. This difference is primarily due to the additional gravitational resistance encountered in the upward direction, which increases the overall pressure drop. As the volume fraction increases, the pressure drop also increases for both flow directions, but the upward flow consistently exhibits a higher pressure drop.

Figure 16 presents the pressure drop (ΔP) versus volume fraction (VF) for a coil diameter of 140 mm. Similar to the 180 mm diameter, the pressure drop in the upward flow is higher than in the downward flow. The gap between the two flows' pressure drops becomes more pronounced at higher volume fractions. The 140 mm diameter coil shows increased sensitivity to volume fraction changes in both flow directions, indicating that the coil diameter significantly influences the pressure dynamics in two-phase flows.

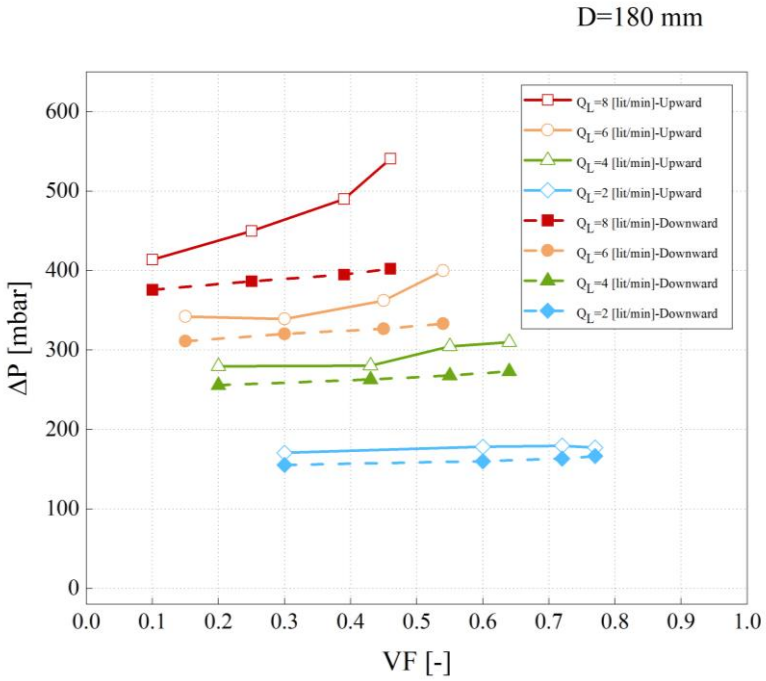

Fig. 15. Variation of ΔP vs. VF for D=180 mm, for upward and downward flow.

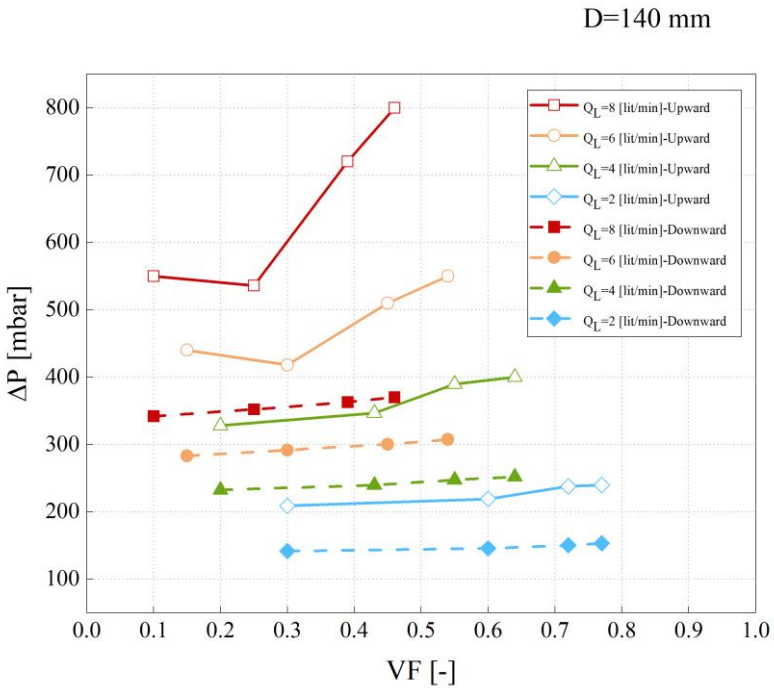

Fig. 16. Variation of ΔP vs. VF for D=140 mm, for upward and downward flow.

In Fig. 17, the pressure drop (ΔP) is plotted against the volume fraction (VF) for a coil diameter of 100 mm. The trend observed is consistent with the larger diameters, where the upward flow exhibits a higher pressure drop compared to the downward flow across all volume fractions. The 100 mm coil diameter shows the highest pressure drop among the three diameters tested, underscoring the impact of reduced coil diameter on increasing flow resistance. The smaller diameter amplifies the effects of both gravitational and frictional forces, resulting in higher pressure drops for both upward and downward flows.

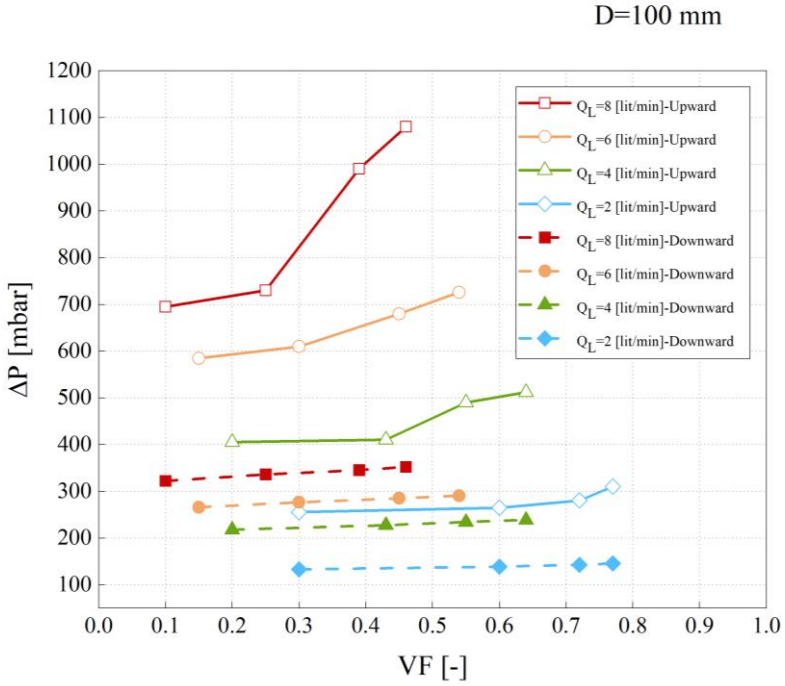

Fig. 17. Variation of ΔP vs. VF for D=100 mm, for upward and downward flow.

4.2. Error analysis

Discordance between actual and observed values is often referred to as the "Observational Error" or the "Measurement Error" in the domains of engineering, physics, and chemistry. Statistical error, on the other hand, encompasses more than just clerical slip-ups in measurement. Because of the intrinsic uncertainty and changeability of random events, any attempt to quantify them is likely to provide inaccurate results. If this were not the case, then such events would not be considered coincidences. The two most common kinds of errors that might occur in a lab are:

- Errors that depend on the measuring tools or the measurement process and are not attributable to random chance are called systematic mistakes. This proves that the measurement method or system is flawed and responsible for the repeated errors.
- Inaccuracies caused by random chance: These occur when the measuring technique is iterated several times. The situation and factors influencing the measurement are the root cause of the inaccuracy in accurately documenting the value of a quantity..

Figure 18 displays the experimental findings and accompanying random error for pressure loss from iterations 49–53. The calculated error, shown as a percentage relative to the original value, is as follows:

$$error\% = \frac{|P_{49-53} - P_{48}|}{P_{48}} \times 100 \quad (4)$$

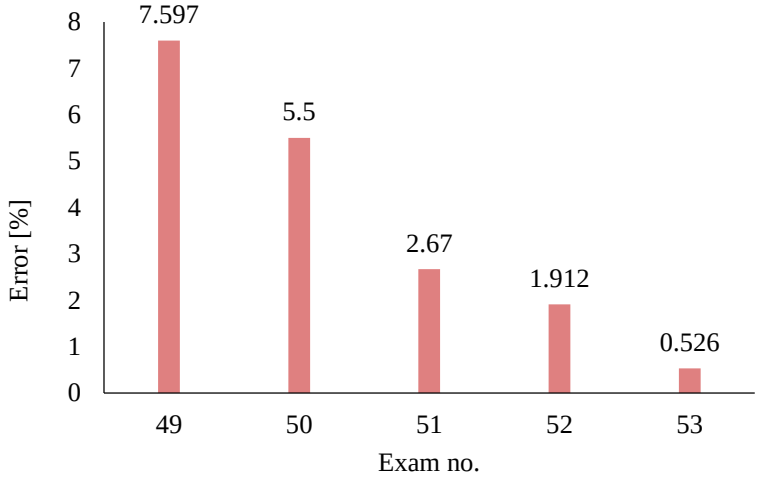

Fig. 18. Error Analysis for downward flow.

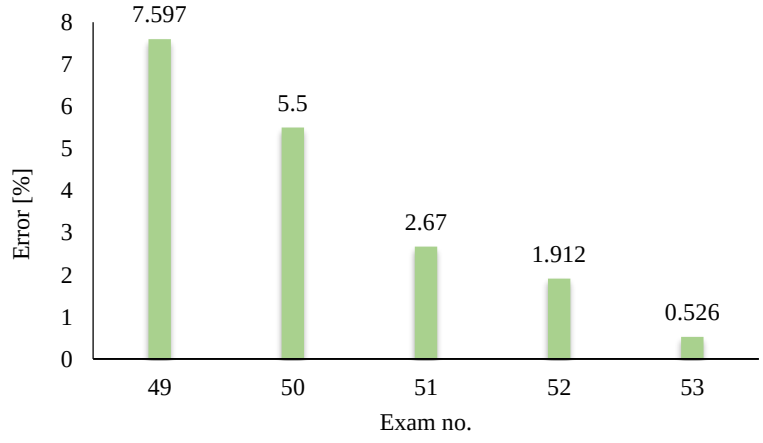

Fig 19. Error Analysis for upward flow.

5. Conclusion

This research investigates the flow of air and water in a helical pipe in both the upstream and downstream directions, focusing on the two-phase nature of the flow. This research uses multiple linear regression to examine test data and ascertain a suitable correlation. The test equipment has a mixing chamber to facilitate the formation of a two-phase flow before it enters the helix. Our primary focus is to examine the influence of various VF and coil sizes on pressure loss. We consider several coils with coil sizes of 100, 140, and 180 mm. The data indicate that decreasing the coil diameter results in lower pressure drop values in downhill flow and greater pressure drop values in upward flow. The results demonstrate that the pressure drop is consistently higher in upward flows compared to downward flows due to gravitational resistance. This effect is more pronounced at smaller coil diameters and higher volume fractions, underscoring the significant influence of coil diameter on pressure dynamics. Both flow directions were compared, revealing that upward flow consistently exhibits greater pressure drops across all tested conditions. The empirical evidence indicates that both the ratio of volume and the physical dimensions of the spiral tube have a significant influence on the reduction in pressure. The interplay between centrifugal forces and the flow regime (downhill vs. uphill) is a critical factor in determining the pressure drop along the tube. These findings are crucial for the optimal design and operation of helical tube systems in various industrial applications. Further research should explore different fluid types and operational conditions to expand the applicability of these correlations.

References

[1] Chingulpitak S, Wongwises S. A comparison of flow characteristics of refrigerants flowing through adiabatic straight and helical capillary tubes. International communications in heat and mass transfer. 2011;38(3):398-404.

[2] Chingulpitak S, Wongwises S. Effects of coil diameter and pitch on the flow characteristics of alternative refrigerants flowing through adiabatic helical capillary tubes. International Communications in Heat and Mass Transfer. 2010;37(9):1305-11.

[3] Zhao Z, Wang X, Che D, Cao Z. Numerical studies on flow and heat transfer in membrane helical-coil heat exchanger and membrane serpentine-tube heat exchanger. International communications in heat and mass transfer. 2011;38(9):1189-94.

[4] Fsadni A, Ge Y, Lamers A. Measurement of bubble detachment diameters from the surface of the boiler heat exchanger in a domestic central heating system. Applied thermal engineering. 2011;31(14-15):2808-18.

[5] Li Z, Jiang S, Yang X, Huang Y, Zhu G, Tu J, et al. Bubbly-intermittent flow transition in helically coiled tubes. Chemical Engineering Journal. 2017;323:96-104.

[6] Mehrabi M, Pesteei S. Modeling of heat transfer and fluid flow characteristics of helicoidal double-pipe heat exchangers using adaptive neuro-fuzzy inference system (ANFIS). International Communications in Heat and Mass Transfer. 2011;38(4):525-32.

[7] Mehrabi M, Pashaee T, Sharifpur M, Meyer JP, editors. Application of Genetic Algorithm-Polynomial Neural Network for Modelling Heat Transfer and Fluid Flow Characteristics of a Double-Pipe Heat Exchanger. Heat Transfer Summer Conference; 2013: American Society of Mechanical Engineers.

[8] Khorasani S, Jafarmadar S, Pourhedayat S, Abdollahi MAA, Heydarpour A. Experimental investigations on the effect of geometrical properties of helical wire turbulators on thermal performance of a helically coiled tube. Applied thermal engineering. 2019;147:983-90.

[9] Khorasani S, Dadvand A. Effect of air bubble injection on the performance of a horizontal helical shell and coiled tube heat exchanger: An experimental study. Applied Thermal Engineering. 2017;111:676-83.

[10] Godbole PV, Tang CC, Ghajar AJ. Comparison of void fraction correlations for different flow patterns in upward vertical two-phase flow. Heat Transfer Engineering. 2011;32(10):843-60.

[11] Khoshvaght-Aliabadi M, Feizabadi A. Compound heat transfer enhancement of helical channel with corrugated wall structure. International Journal of Heat and Mass Transfer. 2020;146:118858.

[12] Moosavi A, Abbasalizadeh M, Dizaji HS. Optimization of heat transfer and pressure drop characteristics via air bubble injection inside a shell and coiled tube heat exchanger. Experimental Thermal and Fluid Science. 2016;78:1-9.

[13] Golmarz TP, Pesteei SM, editors. Investigation of Dean number and curvature ratio in a double-pipe helical heat exchanger. 20th International Conference on Mechanical Engineering-ISME School of Mechanical Eng; 2011.

[14] Haryoko LA, Kurnia JC, Sasmito AP, editors. Forced convection boiling heat transfer inside helically-coiled heat exchanger. IOP Conference Series: Earth and Environmental Science; 2020: IOP Publishing.

[15] Taha T, Cui ZF. CFD modelling of slug flow in vertical tubes. Chemical engineering science. 2006;61(2):676-87.

[16] Murai Y, Inaba K, Takeda Y, Yamamoto F. Backlight imaging tomography for slug flows in straight and helical tubes. Flow Measurement and Instrumentation. 2007;18(5-6):223-9.

[17] Adegoke AS, Oyediran AA. The analysis of nonlinear vibrations of top-tensioned cantilever pipes conveying pressurized steady two-phase flow under thermal loading. Mathematical and Computational Applications. 2017;22(4):44.

[18] Hossain M, Chinenye-Kanu NM, Droubi GM, Islam SZ. Investigation of slug-churn flow induced transient excitation forces at pipe bend. Journal of Fluids and Structures. 2019;1(91):102733.

[19] Akhlaghi M, Mohammadi V, Nouri NM, Taherkhani M, Karimi M. Multi-Fluid VoF model assessment to simulate the horizontal air–water intermittent flow. Chemical Engineering Research and Design. 2019;1(152):48-59

[20] Mimouni S, Fleau S, Vincent S. CFD calculations of flow pattern maps and LES of multiphase flows. Nuclear Engineering and Design. 2017; 1(321):118-31.

[21] Malekzadeh R, Henkes RA, Mudde RF. Severe slugging in a long pipeline–riser system: Experiments and predictions. International journal of multiphase flow. 2012; 1(46):9-21.

[22] Xie C, Guo L, Li W, Zhou H, Zou S. The influence of backpressure on severe slugging in multiphase flow pipeline-riser systems. Chemical Engineering Science. 2017;18(163):68-82

[23] Akgul D, Mercan H, Dalkilic AS. Parametric optimization of heat transfer characteristics for helical coils. Journal of Thermal Analysis and Calorimetry. 2022 Nov;147(22):12577-94

[24] Fan M, Bao Z, Liu S, Huang W. Flow and heat transfer in the eccentric annulus of the helically coiled tube-in-tube heat exchanger used in an aero-engine. International Journal of Thermal Sciences. 2022 ; 1(179):107636.

[25] Dhenge R, Langialonga P, Alinovi M, Lolli V, Aldini A, Rinaldi M. Evaluation of quality parameters of orange juice stabilized by two thermal treatments (helical heat exchanger and ohmic heating) and non-thermal (high-pressure processing). Food Control. 2022;1(141):109150.

[26] Lei Z, Bao Z. Experimental investigation on laminar heat transfer performances of RP-3 at supercritical pressure in the helical coiled tube. International Journal of Heat and Mass Transfer. 2022;1(185):122326.

[27] Xu Z, Liu M, Chen C, Xiao Y, Gu H. Development of an analytical model for the dryout characteristic in helically coiled tubes. International Journal of Heat and Mass Transfer. 2022;1(186):122423.

[28] Moaf M, Alizadeh O, Pendashteh AR. Investigating the Impact of Air Injection on the Thermal Performance of Helical Tube with Varying Helix Diameters: Downward Flow. Iranian Journal of Chemical Engineering (IJChE). 2022;19(2):38-50.

[29] Farhadi F, Eliyassi S. Flow Pattern Identification and Pressure Drop Calculation for Gas-Liquid Flow in a Horizontal Pipeline. Iranian Journal of Chemistry and Chemical Engineering. 1989;8(1):10-9.

[30] ZARE AH, Atashi H, NOUEI S, KHOUSHNOUDI M. Experimental investigation on hydrodynamic and thermal performance of a gas-liquid thermosyphon heat exchanger in a pilot plant. 2008.

[31] ZARE AH, ATASHI H, NOEI S, KHOUSHNOUDI M, KHORAM M, KHOUSHVAGHT M. Experimental and Numerical analysis of flow and heat transfer in a gas-liquid thermosyphon heat exchanger in a pilot plant. 2010. https://doi.org/10.30492/IJCCE.2010.6708.

[32] Wang Y, Zheng W, Guo J, Tian Z, Wang F, Jiang Y, et al. Experimental investigation on the frictional pressure drop of two-phase fluids in the shell side of LNG spiral-wound heat exchangers. Thermal Science and Engineering Progress. 2024;47:102375. https://doi.org/10.1016/J.TSEP.2023.102375.

[33] Khedher NB, Mehryan S, Medani M, Selim MM, Elbashir NB, Boujelbene M. Enhancing the efficiency of a double tube heat exchanger via a novel vibrating woven wire turbulator combined with a helical coiled wire; an experimental study. Applied Thermal Engineering. 2024;248:123121. https://doi.org/10.1016/J.APPLTHERMALENG.2024.123121.

[34] Marzouk S, Abou Al-Sood M, El-Said EM, El-Fakharany MK, Younes M. Study of heat transfer and pressure drop for novel configurations of helical tube heat exchanger: a numerical and experimental approach. Journal of Thermal Analysis and Calorimetry. 2023;148(13):6267-82. https://doi.org/10.1007/S10973-023-12067-7/FIGURES/21.

[35] Kia S, Khanmohammadi S, Jahangiri A. Experimental and numerical investigation on heat transfer and pressure drop of SiO2 and Al2O3 oil-based nanofluid characteristics through the different helical tubes under constant heat fluxes. International journal of thermal sciences. 2023;185:108082 https://doi.org/10.1016/J.IJTHERMALSCI.2022.108082.

[36] Zheng X, Lu X, Gao Y, Jin D, Hu Y, Hu Y, et al. Experimental study on friction pressure drop and circumferential heat transfer characteristics in helical tubes. Frontiers in Energy Research. 2023;11:1204850. https://doi.org/10.3389/FENRG.2023.1204850/BIBTEX.

[37] Kumar A, Saxena V, Deswal H, Kothadia HB. Experimental investigation of pressure drop in helical coil during flow boiling at subatmospheric pressures. Heat and Mass Transfer. 2023;59(10):1855-70. https://doi.org/10.1007/S00231-023-03373-9/FIGURES/11.

[38] Moradi H, Bagheri A, Shafaee M, Khorasani S. Experimental investigation on the thermal and entropic behavior of a vertical helical tube with none-boiling upward air-water two-phase flow. Applied Thermal Engineering. 2019;157:113621. https://doi.org/10.1016/j.applthermaleng.2019.04.031.